Planta (2004) 220: 344–355
DOI 10.1007/s00425-004-1340-4

ORIGINAL ARTICLE

Christian Hermans · Giles N. Johnson
Reto J. Strasser · Nathalie Verbruggen

Physiological characterisation of magnesium deficiency in sugar beet: acclimation to low magnesium differentially affects photosystems I and II

Received: 17 February 2004 / Accepted: 17 June 2004 / Published online: 17 September 2004

Abstract Magnesium deficiency in plants is a widespread problem, affecting productivity and quality in agriculture, yet at a physiological level it has been poorly studied in crop plants. Here, a physiological characterization of Mg deficiency in *Beta vulgaris* L., an important crop model, is presented. The impact of Mg deficiency on plant growth, mineral profile and photosynthetic activity was studied. The aerial biomass of plants decreased after 24 days of hydroponic culture in Mg-free nutrient solution, whereas the root biomass was unaffected. Analysis of mineral profiles revealed that Mg decreased more rapidly in roots than in shoots and that shoot Mg content could fall to 3 mg g^{-1} DW without chlorosis development and with no effect on photosynthetic parameters. Sucrose accumulated in most recently expanded leaves before any loss in photosynthetic activity. During the development of Mg deficiency, the two photosystems showed sharply contrasting responses. Data were consistent with a down-regulation of PSII through a loss of antenna, and of PSI primarily through a loss of reaction centres. In each case, the net result was a decrease in the overall rate of linear electron transport, preventing an excess of reductant being produced during conditions under which sucrose export away from mature leaf was restricted.

Keywords *Beta* · Magnesium deficiency · Mineral profile · Photosynthesis · Sugars

Abbreviations Chl *a, b*: Chlorophyll *a*, *b* · DW: Dry weight · P700: Primary electron donor of photosystem I · PSI, PSII: Photosystem I, II · Q_A: Primary quinone electron acceptor of PSII · RC: Reaction centre

C. Hermans (✉) · N. Verbruggen
Laboratoire de Physiologie et de Génétique Moléculaire des Plantes, Université Libre de Bruxelles, 1050 Brussels, Belgium
E-mail: chermans@ulb.ac.be
Tel.: +32-2-6505412
Fax: +32-2-6505421

C. Hermans · R. J. Strasser
Bioenergetics Laboratory, University of Geneva, 1254 Geneva, Switzerland

G. N. Johnson
Biological School, The University of Manchester, 3.614 Stopford Building, Oxford Road, Manchester, M13 9PT, UK

Present address: C. Hermans
Biology Department, Colorado State University, Fort Collins, CO 80523, USA

Introduction

Magnesium deficiency in plants is a widespread problem, affecting productivity and quality in agriculture (Bennett 1997; Aitken et al. 1999) and forestry (Mitchell et al. 1999). Because Mg has a high hydrated radius, it sorbs less strongly to soil colloids than other cations. It is therefore highly prone to leaching, which is considered as the most important factor reducing Mg availability for roots. Mg deficiency can be brought about by depletion of soil reserves but can also be induced by a failure of the roots to assimilate Mg^{2+}, due to imbalanced competitive inhibition of uptake by calcium and potassium (Mengel and Kirkby 1987).

Plants require magnesium to harvest solar energy and to drive photochemistry. Because of the tendency of Mg to form octahedral complexes, resulting in strong electrophilic axial coordination, Mg is able to occupy a central position in chlorophyll, the pigment responsible for light absorption in leaves (Beale 1999). It has been estimated that the Mg structural pool associated with chlorophyll represents between 15 and 20% of the leaf content (Mengel and Kirkby 1987; Wilkinson et al. 1990). Mg concentration in chloroplastic compartments is modulated by light transition (Wu et al. 1991; Igamberdiev and Kleczkowski 2001) and it has an important

regulatory effect on the activity of enzymes in the Calvin cycle (Pakrasi et al. 2001). In addition to its catalytic role, Mg acts as an allosteric activator of protein complexes (Cowan 2002). Moreover, Mg also plays an important role in the cell energy balance, interacting with the pyrophosphate structure of nucleotide tri- and di-phosphates. The energy-rich compounds Mg-ATP and Mg-ADP represent the main complexed Mg pools in the cytosol, which balance with the free Mg^{2+} pool under the control of adenylate kinase (Igamberdiev and Kleczkowski 2001, 2003).

Although there is substantial literature on Mg uptake and storage in prokaryotes (for review: Kehres and Maguire 2002), only a few reports have been published on the mechanisms of uptake and transport in plants (for review: Shaul 2002; Gardner 2003). Genes for transporters possibly engaged in Mg^{2+} acquisition and partitioning within the plant have been identified in recent years in *Arabidopsis thaliana*. The *AtMHX1* gene cloned by Shaul et al. (1999) codes for an antiporter localised in the vacuolar membrane of the xylem parenchyma cells. Schock et al. (2000) cloned *AtMRS2-1* and *AtMRS2-2* cDNAs, these being homologues of the yeast *MRS2* transporter (Bui et al. 1999). After extended genomic database searches, eight further homologues were identified, *AtMRS2-3* to *AtMRS2-10*, further studied as *AtMGT* (Li et al. 2001). Despite the fact that three members of the plant *MRS2*-like gene family were demonstrated to transport Mg^{2+} into microbes (Schock et al. 2000; Li et al. 2001, reviewed in Gardner 2003), direct evidence of transport function in plants is still lacking.

Few reports exist concerning the effects of a shortage of Mg on physiological processes. Those that do exist describe either an early impairment of sugar metabolism (in bean plants: Fischer and Bremer 1993; Cakmak et al. 1994a, 1994b; in spruce: Mehne-Jakobs 1995; in spinach: Fischer et al. 1998), or a decline in photosynthetic CO_2 fixation rate and stomatal conductance (in pine seedlings: Laing et al. 2000; Sun et al. 2001).

The hierarchy of physiological perturbations is still a matter of debate. It has been proposed that either a decrease in sucrose export is responsible for the inhibition of growth of sink organs (in bean plants: Cakmak at al. 1994b; Marschner et al. 1996) or that a decrease in the metabolic activity in sink organs causes inhibition of sucrose export (in spinach: Fischer et al. 1998). Moreover, the relationship between the decrease in photosynthetic activity and sugar accumulation in source organs has not been established in a whole-plant system.

We have examined the response of sugar beet to Mg starvation, and measured changes in mineral and sugar contents and in photosynthetic parameters relating to photosystem I (PSI) and II (PSII) activities. We showed a differential change in the mineral profile of roots and shoots and an early sucrose accumulation in most recently developed leaves. The rise in leaf sucrose content was followed by acclimation of the photosynthetic apparatus, with distinct responses being observed at the level of the two photosystems.

Materials and methods

Plant material and growth conditions

Seeds of sugar beet (*Beta vulgaris* L. cv. Adonis) were rinsed in distilled water and germinated in peat-based compost. Two weeks after sowing, about 150 plantlets were transferred into 12-l containers for hydroponic culture. The macronutrient composition (in mM) was slightly modified from Cakmak et al. (1994a): 2.00 $Ca(NO_3)_2$, 1.00 $MgSO_4$, 0.88 K_2SO_4, 0.25 KH_2PO_4 and the micronutrient composition (in μM) was 20 FeEDTA, 10 NaCl, 10 H_3BO_3, 1.00 $ZnSO_4$, 1.00 $MnSO_4$, 0.10 $CuSO_4$, 0.01 $(NH_4)_6Mo_7O_{24}$. The pH of the solution was adjusted to 5.8 ± 0.1. At the beginning of the treatment, half the plants were fed with an Mg-free nutrient solution, which was the same as above, except that 1.00 mM $MgSO_4$ was replaced by 1.00 mM Na_2SO_4. Nutrient solutions were replaced every 4 days. The growth conditions in the culture room were 16 h light (250 μmol photons m^{-2} s^{-1})/8 h darkness, temperature 22 ± 2°C and humidity 65 ± 5%.

Sampling

At harvest, plant organs were rinsed in distilled water, and directly dried at 60°C for further mineral analysis or freeze-dried and stored at −80°C for biochemical analysis.

Chemical analysis

1.00 g dried crushed material powder was ashed in a muffle furnace at 450°C. Ashes were digested with 7 N nitric acid and the filtrate assayed for Ca, Mg and Zn by atomic absorption spectrometry at the wavelengths 422.6 nm, 285.2 nm and 213.9 nm, respectively, and for K and Na by atomic emission spectrometry at 404.4 nm and 589.0 nm (AAS 3110; Perkin Elmer).

Sugar analysis

The quantitative determination of soluble and non-soluble sugars was done on extracts from leaf blades. Sugars were extracted using three successive incubations in ethanol (80% v/v) at 85°C. Extraction was assumed to be totally effective after three incubations because a fourth ethanol extraction of the pellets did not contain detectable amounts of glucose. The fraction of soluble sugars was determined spectrophotometrically using an enzyme-linked assay, as described in Sokolov et al. (1998). All enzymes used in this assay were purchased from Roche Diagnostics.

Chlorophyll determination

Pigments were extracted with 80% (v/v) acetone and chlorophyll content was estimated using the method of Porra et al. (1989).

Immunological determination of thylakoid protein

Chloroplasts were extracted after homogenisation in a Polytron flask in 0.4 M sucrose, 0.01 M NaCl, 0.05 M $MgCl_2$, Tricine (pH 7.5) 0.02 M and Na-ascorbate 0.01 M, and centrifugation at 5,000 *g* for 10 min. The pellet was resuspended in 5 mM Tricine (pH 7.9) in order to lyse the chloroplasts. The thylakoid membranes were thereafter resuspended in the same extraction buffer but without Na-ascorbate and with glycerol to reach 1 μg Chl μl^{-1} as a final concentration. The relative content of thylakoid proteins per unit chlorophyll (Chl) was determined immunologically by western blotting. Thylakoids were solubilized as described in Dannehl et al. (1996), and polypeptides were separated by denaturing polyacrylamide gel (12%) electrophoresis using a Mini-Protean II electrophoresis cell (Bio-Rad). Proteins were transferred onto nitrocellulose membrane Hybond-C extra (Amersham Life Science) by electroblotting at 400 mA for 3 h. Primary antibodies against PsbA (dilution 1:2,000) purchased from Agrisera (Sweden) were detected using an anti-chicken IgG–alkaline phosphatase conjugate detection system (Sigma).

Measurement of photosynthetic parameters

PSII fast and slow fluorescence kinetics The behaviour of PSII was assessed through fast fluorescence kinetics (direct induction with 660 nm exposure), recorded with the Plant Efficiency Analyser fluorometer (Hansatech Instruments). The OJIP transients [fluorescence levels F_O (50 μs), $F_{300\mu s}$, F_J (2 ms), F_I (30 ms) and F_M (tF_{MAX}); Strasser et al. 1995] were analysed according to the JIP-test procedure, as previously described (Srivastava et al. 1999; Hermans et al. 2003).

Light response curves were measured with a portable PAM2000 fluorimeter (Walz), on leaf disks in a chamber (LD2/2; Hansatech) with a saturating CO_2 atmosphere, generated by a solution of 1 M $Na_2CO_3/NaHCO_3$ (pH = 9).

PSI absorbance changes The redox state of PSI was monitored as absorbance changes in the near infrared using a Walz PAM 101 fluorometer in combination with an ED-P700DW-E emitter–detector unit (Walz), as described in Golding and Johnson 2003. Signals were recorded on attached leaves in an atmosphere of 2,000 μl l^{-1} CO_2, humidity 95%, light intensity 1,500 μmol photons m^{-2} s^{-1} and temperature 22°C. Leaves were allowed to equilibrate to these conditions within the chamber in darkness for 5 min prior to measurement.

Low-temperature fluorescence measurements Low temperature (77 K) chlorophyll fluorescence spectra were recorded from 600 to 800 nm using an excitation light of 633 nm (He/Ne laser, 20 W m^{-2}) and a multi-branched fiber-optic bundle connected to an S-20 Hamamatsu photomultiplier (R928). Excitation light was defined by a monochromator (H 10 VIS, 0.5-nm slit; Jobin Yvon SAS, Longjumeau, France) equipped with scan controller and the photomultiplier, protected using a red cut-off filter (CS 2-64; Corning). Leaf disks of 0.9 cm diameter were taken from plants dark-adapted for 1 h and were thereafter flash-frozen in liquid nitrogen.

Results

Plant growth and mineral status

After 4 weeks growth in complete mineral solution, Mg deficiency was induced in beet plants at the stage of seven to eight expanded leaves, by transfer to a mineral solution from which Mg was omitted. About 16 days after transfer, the first symptoms of deficiency were observed. Typical interveinal chlorotic areas appeared on the uppermost, expanded leaves of Mg-deficient plants (leaves 10 and 11) and were obvious by day 20. The fresh weight of Mg-deficient plants fell below that of the control from day 20 of treatment (Fig. 1). At day 24, overall biomass was more than one-tenth lower in Mg-deficient plants, this being due to a loss of biomass in the shoots and taproots. Root biomass was unaffected by the treatment (Fig. 1).

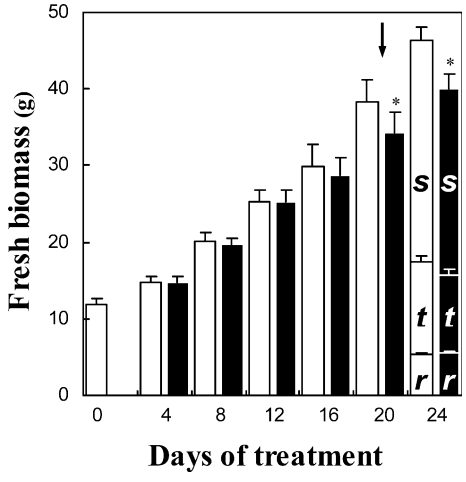

Fig. 1 Sugar beet (*Beta vulgaris*) growth under Mg deficiency. The fresh biomass of individual beet plants was measured throughout the treatment. Mg was omitted from the nutrient solution at day 0, when plants had 7–8 expanded leaves. The biomass allocation between organs is indicated at day 24: *r* root, *t* taproot, *s* shoot. *White columns* control plants, *black columns* Mg-deficient plants. Mean ± SE ($n > 6$). The *arrow* indicates the appearance of obvious chlorosis; *asterisks* (*) indicate a significant difference between treatments at 0.05 level or less

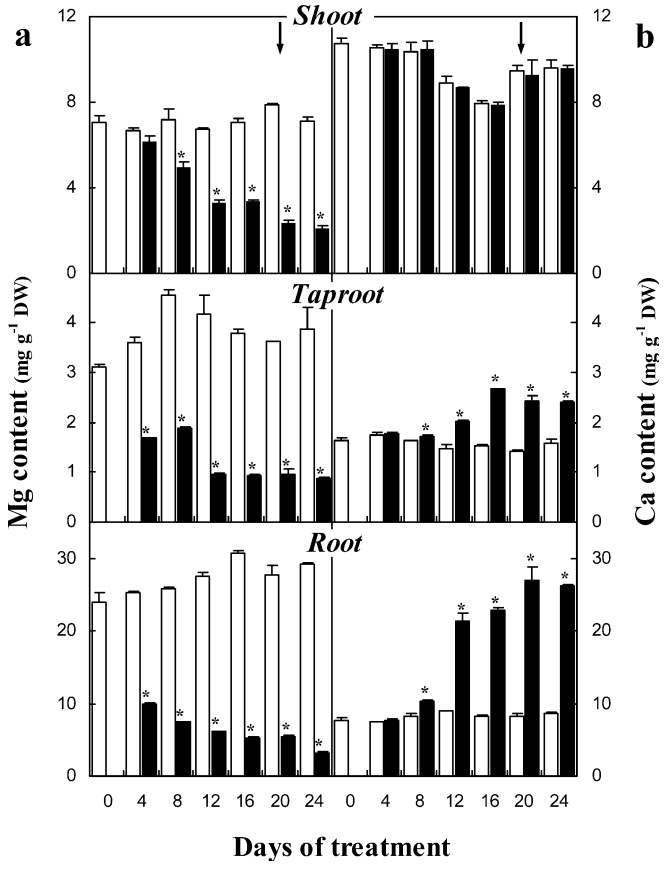

Fig. 2a, b Magnesium and calcium profiles in sugar beet upon Mg deficiency. Mg (**a**) and Ca (**b**) contents in root, taproot and shoot are expressed on a dry-weight basis. Mg was omitted from the nutrient solution of Mg-deficient plants at day 0. *White columns* control plants, *black columns* Mg-deficient plants. Bars represent SE of 3 mineralisations from a pooled powder of 5–10 plants. The *arrow* indicates the appearance of obvious chlorosis; *asterisks* (*) indicate a significant difference between treatments at 0.05 level or less

During the treatment, the Mg content was followed in roots, taproots and shoots in control and Mg-deficient plants (Fig. 2a). The reduction in the Mg content in roots and taproots was abrupt and considerably larger than in shoots. A significant decrease ($P \leq 0.05$) was first observed in the roots and the taproots after 4 days of treatment and in the shoots after 8 days. After 24 days, at the end of the treatment, the Mg contents in the roots and taproots of treated plants were less than a quarter of control values (Fig. 2a, Table 1); the contents of blades and petioles of the fully expanded leaves fell to below a fifth of control values; and the Mg contents of blades and petioles in young leaves were a quarter of the control value (results not shown). The average total Mg pool in individual plant was estimated to be 10 mg at day 0 of treatment (Fig. 3). At the end of the treatment, an individual control plant had accumulated 43.2 mg Mg on average, while the initial content was maintained in Mg-deficient plants. This confirmed that the Mg-free nutrient solution was not contaminated with any external Mg source during the treatment. The distribution of Mg between organs was altered within 4 days of treatment and held until the end of the experiment. After 4 days of Mg starvation, the proportion of Mg in roots, taproots and shoots represented, respectively, 9, 8.5 and 82.5% of the total Mg pool of the plant (Fig. 3a), while these proportions were 17, 13.5 and 69.5% (Fig. 3b) in the control plants.

The contents of other minerals were also measured (Fig. 2b, Table 1) and the most relevant results are presented. An increase in calcium content was apparent in Mg-deficient plants, especially in roots and taproots, where levels up to three times the control were observed (Fig. 2b). The total Ca content of the aerial biomass of Mg-deficient plants was not affected, although a more-detailed analysis revealed that Ca contents were half of control values in the blades and nearly doubled in the petioles of mature leaves (Table 1). Potassium content increased slightly in all organs, except in the youngest parts of the plant, where the K content was similar to the control value (results not shown). The content of sodium (the substitution cation) rapidly increased by up to as much as 10-fold the control content. Zn content gradually increased in the roots and taproots and decreased

Table 1 Mineral profile at day 24 in sugar beet (*Beta vulgaris*) upon Mg deficiency

		Mg	Ca	K	Na	Zn
Mineral content in organs[a]						
Root	Control	14.56 ± 0.17	04.30 ± 0.07	34.6 ± 0.4	00.79 ± 0.02	106.8 ± 0.2
	Mg deficiency	03.26 ± 0.04	13.09 ± 0.15	46.1 ± 0.5	7.50 ± 0.06	168.1 ± 0.4
Taproot	Control	03.88 ± 0.42	01.57 ± 0.10	16.1 ± 0.0	00.17 ± 0.01	11.1 ± 1.4
	Mg deficiency	00.88 ± 0.02	02.41 ± 0.02	19.8 ± 0.2	01.59 ± 0.01	14.7 ± 1.1
Blade[b]	Control	11.46 ± 0.23	20.66 ± 0.63	57.9 ± 4.2	01.72 ± 0.03	51.5 ± 1.0
	Mg deficiency	02.18 ± 0.22	07.90 ± 0.56	70.0 ± 4.2	13.11 ± 0.48	36.8 ± 1.6
Petiole[b]	Control	03.64 ± 0.02	07.07 ± 0.12	43.9 ± 2.9	00.49 ± 0.02	10.5 ± 0.8
	Mg deficiency	00.51 ± 0.03	12.81 ± 0.38	55.8 ± 1.2	09.70 ± 0.42	17.9 ± 1.0
Total mineral pool in plant[c]						
	Control	43.2	44.0	266.5	7.2	213.0
	Mg deficiency	10.0	45.0	277.1	42.9	198.0

[a]Mg, Ca, K, Na: mg g^{-1} DW; Zn: μg g^{-1} DW. Mean of 3 mineralisations from a pooled powder of 5–10 plants ± SE
[b]From fully expanded leaves
[c]Estimated from the mineral content average and the dry weight average of root, taproot and shoot. Mg, Ca, K, Na: mg and Zn: μg

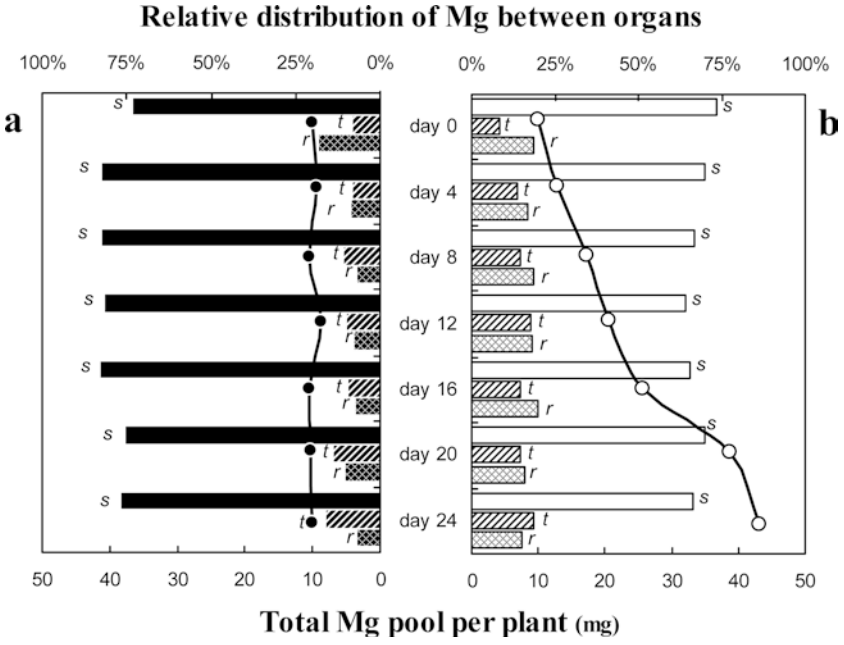

Fig. 3a, b Magnesium allocation to organs in sugar beet upon Mg deficiency. Relative distribution of Mg between plant organs and total Mg pool (mg) per plant, as a function of the days without (**a**) or with (**b**) Mg supply in the nutrient solution. Mg contents in the shoot (*s*), taproot (*t*) and root (*r*) are expressed as a percentage of the estimated total Mg pool in the plant

in blades and the petioles of Mg-deficient plants (Table 1).

Carbohydrate status

Sucrose and glucose contents were measured in uppermost fully expanded blades after 16 h of light throughout the Mg-deficiency treatment. Sucrose accumulation was detected after 12 days, and the sucrose content was more than three times greater than the control by the end of the experiment (Fig. 4a). Glucose started to increase after 16 days in Mg-deficient blades (Fig. 4b), but to a lesser extent than sucrose.

Photosynthesis

Mg deficiency resulted in a loss of chlorophyll from the uppermost fully expanded leaves after 17 days of treatment, with over half of all chlorophyll being lost by the end of the experiment (Fig. 5a). Chlorophylls *a* and *b* were not lost equally, with Chl *b* starting to decrease first, followed later by Chl *a*. The relative content of PsbA (D1 in PSII) protein was determined by western analysis (Fig. 5b). A major band (25 kDa) and a minor heavier band (above 25 kDa), separated by LHCII complexes (coloured protein–pigment complexes that were not dissociated), were clearly apparent on the blotting membrane. Usually, the molecular weight of PsbA protein after SDS–PAGE is reported to be 39 kDa, but the protein may migrate at a smaller apparent size due to processing and migration conditions. On a total-chlorophyll basis, the amount of PsbA proteins was not altered in Mg-deficient samples compared to control ones until the end of the treatment (Fig. 5b).

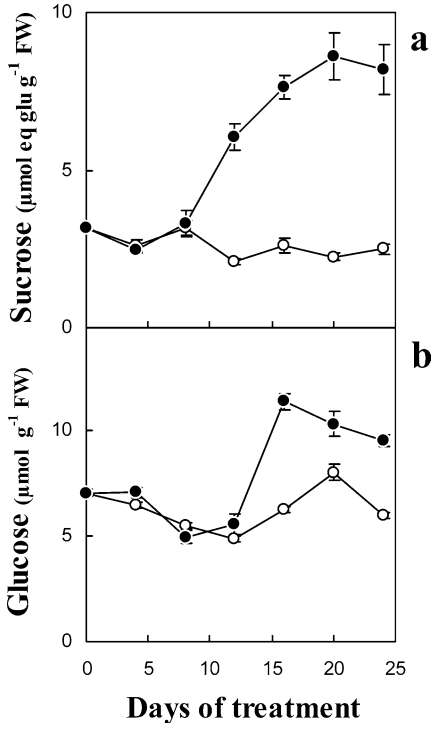

Fig. 4a, b Sugar contents in sugar beet leaves upon Mg deficiency. Sucrose (**a**) and glucose (**b**) contents were measured in the uppermost expanded blades after 16 h of light. Mean of 3 extractions from a pooled sample of 5 plants ± SE. Mg was omitted from the nutrient solution at day 0

Measurements of photosynthetic parameters were performed on the uppermost fully expanded leaves throughout the treatment. Parameters referring to pho-

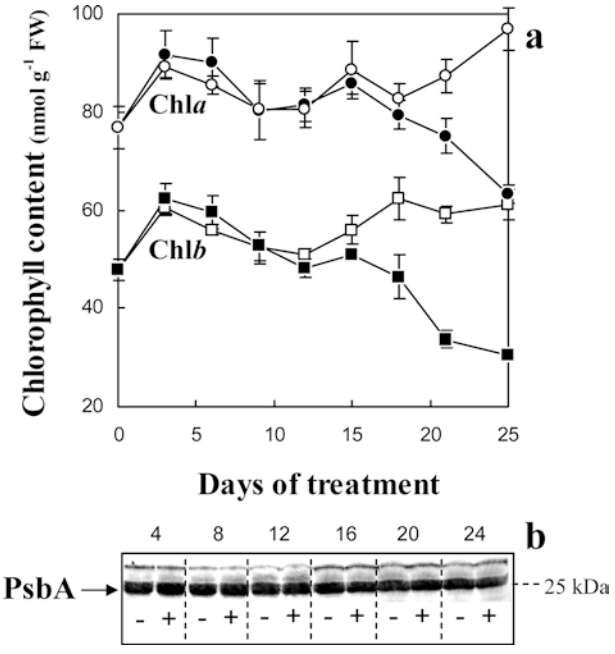

Fig. 5a, b Chlorophyll and PsbA protein contents in sugar beet leaves upon Mg deficiency. **a** Chlorophyll content (*circles* Chl *a*, *squares* Chl *b*) in uppermost expanded leaves as a function of the growth with or without Mg in the nutrient solution. *Open symbols* control plants, *closed symbols* Mg-deficient plants. Means of 5 replicates ± SE. **b** Immunoblot analysis of PsbA (D1 protein) of PSII in control (+) and Mg-deficient (−) plants. Thylakoid membrane extracts corresponding to 3.5 µg of total chlorophyll were loaded in each lane

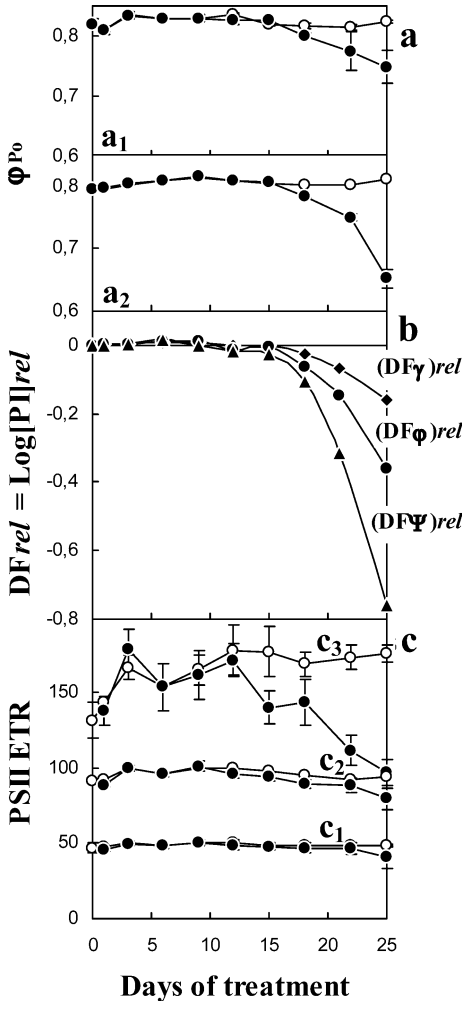

Fig. 6a–c Variation of PSII parameters in sugar beet leaves upon Mg deficiency. **a** Maximal quantum efficiency of PSII (ϕ_{Po}) measured with a direct system (a_1) and modulated system (a_2). Bars represent SE: $n \geq 32$ (a_1) and $n = 5$ (a_2). **b** Evolution of the components of the PSII driving force. The three additive components are $(DF\gamma)rel = \text{Log}\,[\gamma/(1-\gamma)]_{rel} = \text{Log}\,[\gamma/(1-\gamma)]_{Mg\ def} - \text{Log}\,[\gamma/(1-\gamma)]_{Control}$; $(DF_\phi)rel = \text{Log}\,[\phi_{Po}/(1-\phi_{Po})]_{rel} = \text{Log}\,[\phi_{Po}/(1-\phi_{Po})]_{Mg\ def} - \text{Log}\,[\phi_{Po}/(1-\phi_{Po})]_{Control}$; $(DF\Psi)rel = \text{Log}\,[\Psi_o/(1-\Psi_o)]_{rel} = \text{Log}\,[\Psi_o/(1-\Psi_o)]_{Mg\ def} - \text{Log}\,[\Psi_o/(1-\Psi_o)]_{Control}$. $DF\gamma$ is a measure of the density of active reaction centres per chlorophyll, DF_ϕ is a measure of the force of the light reactions, DF_Ψ is a measure of the dark reactions after Q_A-, expressed as the log of the fraction of electrons leaving Q_A- divided by the fraction of electrons remaining on Q_A-. $\Delta DF = \text{Log}[PI_{ABS}]rel = (DF\gamma)rel + (DF_\phi)rel + (DF_\Psi)rel$. Mean of 30–40 measurements. **c** Electron transport rate of PSII (*PSII ETR*) measured at three light intensities: 70 (c_1), 150 (c_2) and 1,700 µmol photons $m^{-2}\ s^{-1}$ (c_3). Bars represent SE of 5 values. Mg was omitted from nutrient solution at day 0. *Open circles* control plants, *closed circles* Mg-deficient plants

tosystem kinetics are derived from the equations in the Appendix. To assess PSII activity, the fast and slow Chl *a* fluorescence kinetics at room temperature were followed. The maximum quantum yield for primary photochemistry of PSII (ϕ_{Po} or F_V/F_M), related to the PSII dark-adapted state, was measured both with a direct induction fluorometer and a modulated fluorometer (see Materials and methods). A decrease in F_V/F_M was observed after 18 days of treatment in Mg-deficient leaves when measurements were done with each apparatus (Fig. 6a). At day 25, F_O had increased by one-tenth and F_M decreased by one-fifth relative to the control, giving a decrease in F_V/F_M. In order to characterise further the effects of Mg deficiency on PSII, a variety of parameters was calculated, based on the OJIP fast fluorescence induction curve (Strasser et al. 1995; Hermans et al. 2003). The structure and function of PSII have been described through the performance index (PI_{ABS}). Due to the exponential behaviour of PI_{ABS}, the driving force (DF) has been defined as log PI_{ABS}. Three additive components building DF (DF_γ, DF_ϕ and DF_Ψ) are plotted in Fig. 6b. DF started to decrease after 18 days of treatment in Mg-deficient leaves, mainly due to a decrease in the component referring to the electron transport (DF_Ψ).

Light response curves related to PSII activity were estimated using a modulated fluorometer at six different light intensities ranging from 70 to 1,700 µmol photons $m^{-2}\ s^{-1}$. Changes in the quantum yield of PSII primary photochemistry (Φ_{PSII}) at any given light intensity were observed starting around day 15, implying a loss of PSII electron transport across all light intensities. The relative rates of electron transport of PSII (PSII ETR) were plotted for three different light intensities (Fig. 6c). The PSII ETR values at 1,700 and

990 μmol photons m^{-2} s^{-1} started to decrease after 15 days, but were less affected at light intensities lower than 550 μmol photons m^{-2} s^{-1}.

The redox state of the primary electron donor of PSI (P700) was monitored by near-infrared absorption spectroscopy. The maximum signal ΔS_{MAX} in the near-infrared region induced by a saturating far-red light of 10 s (as described in Weis and Lechtenberg 1988), equated to the total P700 pool in the leaf. ΔS_{MAX} started to decrease after 15 days of treatment in Mg-deficient plants, falling to below half of the control value after 18 days of the treatment (Fig. 7a). Measurements of the kinetics and amplitude of the near-infrared absorbance signal were measured following a light-to-dark transition at steady state. The amplitude of this signal (ΔS), corresponding to $P700^+$ accumulated in the light, decreased in Mg-deficient plants by only one-tenth at the end of the treatment (Fig. 7a). Exponential decay curves were fitted to determine the first-order rate constant (k) for re-reduction of P700 (Ott et al. 1999; Clarke and Johnson 2001; Golding and Johnson 2003). The rate of PSI electron transport calculated on a total-P700 basis (PSI ETR_{total}) fell by approximately one-fifth during the treatment (Fig. 7b). The rate of PSI electron per P700 oxidised fraction (PSI $ETR_{per\ RC}$) nearly doubled in Mg-deficient plants by day 25 (Fig. 7c). Flash-induced kinetics were also measured on light-adapted plants during a 100-ms saturating light pulse exposure (Clarke and Johnson 2001). ΔS was unaffected until day 21 in Mg-deficient plants, when it decreased to half the control value, although the rate constant k was not affected or slightly decreased at the end of the treatment (results not shown).

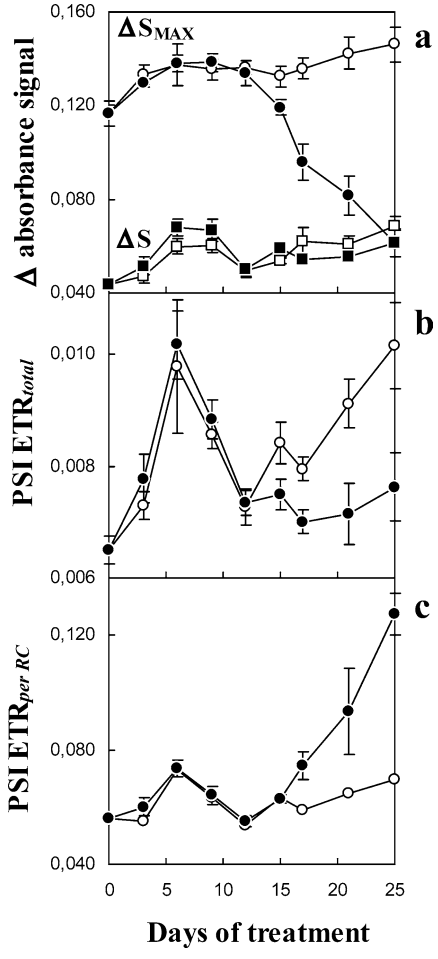

Fig. 7a–c Variation of PSI activity parameters in sugar beet leaves upon Mg deficiency. **a** Difference in absorbance signals of PSI (820 nm). *Circles* ΔS_{MAX}, corresponding to the signal amplitude induced by far-red light on dark-adapted samples; *squares* ΔS, corresponding to the signal amplitude following a light-to-dark transition on samples adapted to 1,500 μmol photons m^{-2} s^{-1} light. **b** Electron transport rate of PSI on a total-P700 basis (PSI ETR_{total}) measured on samples adapted to 1,500 μmol photons m^{-2} s^{-1}. **c** Electron transport rate of PSI expressed per P700 oxidised fraction (PSI $ETR_{per\ RC}$) measured on samples adapted to 1,500 μmol photons m^{-2} s^{-1}. *Open symbols* control plants, *closed symbols* Mg-deficient plants. Bars represent SE of 5–12 measurements. Mg was omitted from nutrient solution at day 0

Chlorophyll fluorescence emission spectra of leaf disks excised from dark-adapted leaves were recorded at 77 K between 650 and 800 nm using a 633-nm excitation light (Fig. 8). At low temperature, PSI fluorescence is enhanced and the emission spectra show distinct bands. The emission maxima at 685 and 695 nm are attributed to PSII core antennae (CP43 and CP47) with a minor contribution from the PSII light-harvesting complex, LHCII, while the maximum at 730 nm is due to PSI

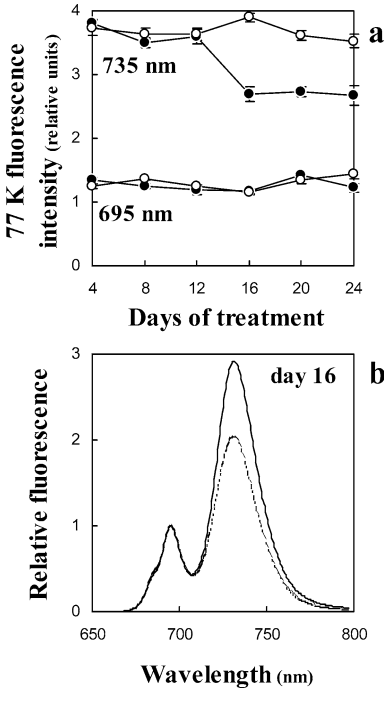

Fig. 8a, b Low-temperature fluorescence emission spectra in sugar beet leaves upon Mg deficiency. **a** Evolution of the peaks at 695 nm and 735 nm from recorded spectra. *Open circles* control plants, *closed circles* Mg-deficient plants. Mean of 7 measurements ± SE. Mg was omitted from nutrient solution at day 0. **b** 77 K fluorescence spectra (normalized to the 695 nm peak) at day 16 of treatment for control (*unbroken trace*) and Mg-deficient (*dashed trace*) plants. Average of 7 spectra

antennae. In uppermost expanded leaves, the maximum at 731 nm started to decrease after 16 days of Mg-deficiency treatment, falling to 70% of the control value (Fig. 8a,b). No relative spectral changes in the fluorescence emission from 690 to 710 nm were observed, except at the end of the treatment.

Discussion

Effect of Mg deficiency on plant growth and mineral status

Among environmental factors, mineral nutrition is a major determinant of biomass allocation in plants (Marschner et al. 1996; López-Bucio et al. 2003). In this study, Mg deficiency induced a decrease in the fresh weight of plants, mainly through a reduction of the shoot biomass (Fig. 1). The effects of Mg deficiency on plant growth are expected to be complex in view of the large number of Mg-requiring enzymes (Cowan 2002) that are involved in energetic metabolism. However, a possible change in Mg-adenylate species equilibrium could account in part for the observed unrestricted root growth. At low [Mg^{2+}], the binding of Mg by ATP is more efficient than by ADP, and therefore an enrichment of Mg-complexed ATP compared to Mg-complexed ADP content occurs (Igamberdiev and Kleczkowski 2001, 2003). As most metabolic enzymes utilizing Mg-ATP are inhibited by Mg-ADP in a competitive way, the rate of metabolic flux in roots may be even higher under Mg^{2+} depletion because of a higher Mg-ATP/Mg-ADP ratio (Igamberdiev and Kleczkowski 2003). Likewise, it was previously reported in Pi-deficient bean plants that root growth was unaffected and the adenylate metabolism was altered (Rychter et al. 1992).

Removal of Mg from the growth medium led to a decrease in Mg in all parts of the plant, this being most abrupt in roots and taproots (Fig. 2a). Actually, the partitioning of Mg between cell compartments or within the plant may be partially fulfilled by antiporters for which efflux activities have been measured (Pfeiffer and Hager 1993; Amalou et al. 1994), or genes already cloned, like *AtMHX* in *Arabidopsis* (Shaul et al. 1999). Interestingly, Shaul et al. (1999; reviewed in Shaul 2002) proposed that AtMHX could determine the proportion of absorbed Mg^{2+} between tonoplast and cytosol of the xylem parenchyma cells at the root vascular cylinder. Therefore, this antiporter could serve in a buffering role, sequestering Mg^{2+} in excess of that which could be loaded into xylem, or establishing a vacuolar pool for use upon deficiency. An AtMHX1 orthologue in sugar beet may be involved in the change of Mg partitioning that was observed here between shoot and root during Mg deficiency (Figs. 2a, 3a,b).

When Mg supply to the roots is insufficient, recycling of Mg is required to cover the growth of newly developing organs. Here, beet plants could cope with 3 mg g^{-1} DW in the shoot for 16 days, without any visual symptoms or decrease in biomass (Fig. 1). Clearly, the incidence of Mg deficiency was attenuated by the initial amount of Mg present within the plant, which could be mobilized to newly developed tissues (Fig. 3a,b, Table 1). Mg is a mobile element within the plant (Mengel and Kirkby 1987; Marschner et al. 1996) and is typically ranked as the first divalent cation in term of abundance in the phloem sap (Pate et al. 1998; Peuke et al. 2002).

Influence of Mg substitution on plant metabolism and the profile of other minerals

The way in which salt substitutions are made in order to induce Mg deficiency may considerably modify the assimilation and partitioning of other elements. Different substitutions have been applied in previous studies, resulting in variation in the concentrations of major elements (Terry and Ulrich 1974; Fischer and Bremer 1993; Dannehl et al. 1996; Fischer et al. 1998; Sun et al. 2001). In order not to alter the anion/cation balance, equimolecular amounts of sodium sulfate were used, as in Cakmak et al. (1994a, 1994b). Substitution using potassium sulfate resulted in similar physiological responses (appearance of symptoms and severity of the stress) to those using sodium sulfate substitution (results not shown). The 2 mM Na^+ difference between nutrient solutions was reflected by higher Na contents in Mg-deficient plants (Table 1). Nevertheless, sugar beet is considered as a natrophilic crop plant (Marschner 1995). From previous reports, NaCl concentrations even in the range of 50 mM did not cause any growth reduction in beet plants (Ghoulam et al. 2002). However, addition of 8.7 mM NaCl was able to counteract the impact of low Mg supply in *Pinus radiata* by increasing the rate of net photosynthesis and biomass production of stem and roots (Sun et al. 2001).

In the absence of Mg^{2+} in the nutrient solution, an increased uptake of other cations was observed. The tendency to compensate the charge balance of a missing ion in the nutrient solution by the enhanced uptake of others is frequently reported (Peuke et al. 2002). Here, this phenomenon was mainly apparent for calcium and to a lesser extent for potassium (Fig. 2b, Table 1). Ca uptake considerably increased in Mg-deficient root parts (Fig. 2b) and in petioles, and decreased in blades (see Table 1). In a previous study of Terry and Ulrich (1974), Ca contents in blades and petioles of beet leaves increased after 1 week of treatment, but were thereafter lower and similar to control values. Similarly, low Mg supply increased Ca and K contents in leaves of sunflower plants (Lasa et al. 2000) and a K–Mg antagonism was reported in K-deficient tomato plants (Pujos and Morard 1997). The observed increase of K content in beet plants may also be linked to the propensity of K to form strong complexes with nucleotides, which can be expected to participate in adenylate kinase equilibrium

(Blair 1970), while Mg concentration decreases. The total Zn content in plants did not change upon Mg deficiency; however, the root content increased and the shoot content decreased (Table 1). Shaul et al. (1999) have shown that AtMHX1 was also transporting Zn^{2+} in *Arabidopsis thaliana*. As it is possible that an orthologue of that gene exists in sugar beet, a preferential retention of Zn during Mg deficiency in the vacuoles of root and stem xylem parenchyma cells could have discriminated against Zn translocation to the blade tissues.

Photosynthetic acclimation during Mg deficiency

In the hierarchy of physiological disturbances occasioned by Mg deficiency, sucrose (and later glucose) accumulated in leaf blades (Fig. 4a,b) before any loss in chlorophyll content (Fig. 5a) or photosynthetic activity (Figs. 6a–c, 7a–c) could be measured. Therefore, the increase in sucrose content could have triggered a decline in photosynthesis. Obviously, sucrose is not just a passive carrier molecule for long-distance transport. In the literature, a negative correlation is generally reported between sugar levels, photosynthetic activities, chlorophyll content and expression of photosynthetic genes (see Foyer 1988; Sheen 1990; Oswald et al. 2001; Wingler et al. 2004).

One of the earliest signs of Mg deficiency impacting on photosynthesis was a decline in the concentration of Chl *b*, relative to the control, followed by a loss of Chl *a* (Fig. 5a). Given that Chl *b* is mostly associated with LHCII, the light-harvesting complex of PSII, this change was probably indicative of a relative loss of PSII peripheral antenna, or, alternatively, of a change in photosystem stoichiometry in favour of PSI. In support of the first hypothesis, Mg-deficient *Arabidopsis thaliana* leaves contain smaller amounts of LHCII and disorganized thylakoid membranes (Lu et al. 1995). Clearly, Mg^{2+} is required for thylakoid grana stacking (Kaftan et al. 2002) and LHCII also participates in that cation-mediated formation of grana, besides serving as the major antenna for PSII.

A decrease in the maximum quantum yield for primary photochemistry of PSII (ϕ_{Po}), measured on dark-adapted leaves, was observed (Fig. 6a) in association with a loss of chlorophyll (Fig. 5a). Chlorophyll *a* fast fluorescence kinetics have previously been investigated in *Pinus radiata* seedlings (Sun et al. 2001). Here, a more detailed analysis of Chl *a* fast fluorescence induction using the JIP-test approach (Strasser et al. 1995), provided an extended range of parameters to assess the effects of Mg deficiency on PSII. This approach allowed us to show that electron transfer beyond the primary quinone electron acceptor of PSII, Q_A, is affected earlier and to a greater extent than the light reactions or the density of active reaction centres (RCs) per chlorophyll (or absorption ABS) or per leaf area (or cross-section; Fig. 6b; see Appendix). These data are consistent with a previous study of spinach suffering from Mg and S deficiency (Dannehl et al. 1996). Feedback regulation of photosynthesis could also occur from redox signals. Some studies have indicated that the redox status of carriers in the electron-transport chain or other stromal components exerts a control over photosynthetic gene expression (Oswald et al. 2001; Surpin et al. 2002).

Shortly after the increase in sucrose content in leaves, the efficiency of PSII achieved under steady-state illumination began to decline (Fig. 6c). Given the loss of antenna implied by changes in chlorophyll content (Fig. 5a), the rate of PSII electron transport probably declined more than that indicated by fluorescence estimates, since part of the PSII cross-sectional area was likely to be lost. Western blot analysis did not indicate any loss of PSII core complex, per unit chlorophyll (Fig. 5b), implying that the main mechanisms giving rise to a loss of PSII activity were the loss of light-harvesting capacity and an inhibition of the electron-transport chain after PSII.

At the level of PSI, the most marked effect was a decrease in ΔS_{MAX}, the maximal reflectance signal at 830 nm induced by exposure to far-red light (Fig. 7a). Although such measurements need to be interpreted with caution, the most likely explanation for the decrease in the signal would be a loss of total PSI centres occurring per unit area of leaf. The use of a dual-wavelength pulse-modulation system makes measurements quite specific to P700, reducing contributions from light scattering and also from plastocyanin or ferredoxin (Klughammer and Schreiber 1991; Kramer and Crofts 1996). The total concentration of P700 oxidised under steady-state conditions ($\sim\Delta S$) remained largely constant during most of the treatment (Fig. 7a). Calculations of PSI electron transport per total P700 (calculated as the product of the A_{830} signal upon a light-to-dark transition and the rate constant for that reduction) fell relative to the control, from day 15 (Fig. 7b), probably reflecting a limitation in the pool of PSI available to take part in electron transport. By contrast, calculations of PSI electron transport per P700 oxidised fraction increased relative to the control, from day 17 (Fig. 7c). In addition, the 731-nm peak of normalized low-temperature fluorescence spectra (Fig. 8a,b) was severely decreased relatively to PSII in Mg-deficient plants after 16 days of treatment. This observation was consistent with a pronounced reduction of the antenna and core of PSI. In an attempt to characterize the PSI reaction centre, western blot analyses were performed with polyclonal anti-PsaA antibody, however without success.

In conclusion the two photosystems showed sharply contrasting responses to Mg deficiency, after sugars had begun to accumulate. PSII was probably down-regulated largely through a loss of antenna, and PSI through a loss of reaction centres. The reduction of LHCII size will reduce the rate of light absorption, so reducing the turnover of the reaction centres under limiting light

conditions, as LHCII represents an important component of the total antenna system of PSII. In contrast, much less of the total PSI antenna is associated with LHCI (Jensen et al. 2003, and references therein) than in the case for PSII/LHCII. Therefore, reducing the amount of PSI core complexes would be a more effective strategy than a reduction of LHCI antenna. In each adaptation strategy, the end result would be to lower the overall rate of linear electron transport between photosystems so as to prevent an excess of reductant being produced during conditions in which sugar export away from the leaf was restricted (our unpublished results).

Acknowledgements C. Hermans was supported by a grant from Fonds pour la Formation de la Recherche dans l'Industrie et dans l'Agriculture. This research was supported by grant from the Interuniversity Attraction Pole Program—Belgian Science Policy (Project V/13). Part of the experimental work was done during a Marie Curie Studentship Training Site program at the Biological School of The University of Manchester. Access to the spectrometer equipment was provided by Prof. C. Buess, Laboratoire de Chimie Analytique, Université Libre de Bruxelles.

Appendix: definition of photosynthetic parameters

PSII fluorescence parameters

Maximum quantum yield for primary photochemistry at time zero

(Butler and Kitajima 1975; Kitajima and Butler 1975)

$$\varphi_{Po} = 1 - (F_O/F_M)$$

Actual quantum yield for primary phytochemistry at time t

(Paillotin 1976)

$$\varphi_{Pt} = 1 - (F_t/F_M) = (F_V/F_M)(1 - V_t) = (F_M - F_t)/F_M$$

where relative variable fluorescence at the state t is given by $V_t = (F_t - F_O)/(F_M - F_O)$

Actual quantum yield for primary photochemistry at steady state under a given light condition

(Genty et al. 1989)

$$\varphi'_{PS} = 1 - \left(F'_S/F'_M\right) = F'_V/F'_M\left(1 - V'_S\right) = \left(F'_M - F'_S\right)/F'_M = \Phi_{PSII}$$

where $'$ refers to the light-adapted state, and relative variable fluorescence at the various states is given by $V_S' = (F_S' - F_O')/(F_M' - F_O')$.

Rate of electron transport

$$\text{PSII ETR} = \Phi_{PSII}{*}\text{PFD}$$

Performance index (PI) and driving force (DF) of PSII

(Hermans et al. 2003)

$$\begin{aligned} \text{PI}_{ABS} &= [\gamma/(1-\gamma)] * [\varphi_{Po}/(1-\varphi_{Po})] * [\Psi_o/(1-\Psi_o)] \\ &= \left\{\left[\left(F_{300\,\mu s} - F_{50\,\mu s}\right)/\left(F_{2\,ms} - F_{50\,\mu s}\right)\right] * (F_M/F_V)\right\} \\ &\quad * [F_V/F_O] * [(F_M - F_{2\,ms})/(F_{2\,ms} - F_O)] \end{aligned}$$

$$\text{DF} = \text{Log}(\text{PI}_{ABS}) = \text{DF}_\gamma + \text{DF}\varphi + \text{DF}_\Psi$$

where:

$$\gamma = \text{Chl}_{RC}/\text{Chl}_{tot} = \text{RC}/(\text{ABS} + \text{RC})$$

$$\varphi_{Po} = \text{TR}/\text{ABS}$$

$$\Psi_o = \text{ET}/\text{TR}$$

PSI absorbance parameters

Maximum signal amplitude induced by far-red light on dark-adapted leaves

(Weis and Lechtenberg 1989)

$$\Delta S_{MAX} \sim (\text{P700})\text{total}$$

Signal amplitude following a light-to-dark transition on light-adapted leaves

(Weis and Lechtenberg 1989)

$$\Delta S \sim \text{P700}^+$$

Rate of PSI electron transport calculated on a total P700 basis

(Clark and Johnson 2001)

$$\text{PSI ETR}_{total} = (\Delta S){*}k$$

Rate of PSI electron transport per P700 oxidised fraction

(Ott et al. 1999)

$$\text{PSI ETR}_{per\ RC} = (\Delta S/\Delta S_{MAX}){*}k$$

where k is the rate constant for P700 re-reduction.

References

Aitken RL, Dickson T, Hailes KJ, Moody PW (1999) Response of field-grown maize to applied magnesium in acidic soil in north-eastern Australia. Aust J Agric Res 50:191–198

Amalou Z, Gibrart R, Trouslot P, d'Auzac J (1994) Solubilization and reconstitution of the $Mg^{2+}/2H^+$ antiporter of the lutoid tonoplast from *Hevea brassiliensis* latex. Plant Physiol 106:79–85

Beale SI (1999) Enzymes of chlorophyll biosynthesis. Photosynth Res 60:43–73

Bennett WF (1997) Nutrients deficiencies & toxicities in crop plants. APS Press, The American Phythopathological Society, St. Paul, MN, USA

Blair JM (1970) Magnesium, potassium and the adenylate kinase equilibrium. Magnesium as a feedback signal from the adenine nucleotide pool. Eur J Biochem 13:384–390

Bui DM, Gregan J, Jarosch E, Ragnini A, Schweyen JR (1999) The bacterial magnesium transporter CorA can functionally substitute for its putative homologue Mrsp2p in the yeast inner mitochondrial membrane. J Biol Chem 274:20438–20443

Butler WL, Kitajima M (1975) Fluorescence quenching in photosystem II of chloroplasts. Biochim Biophys Acta 376:116–125

Cakmak I, Hengeler C, Marschner H (1994a) Partitioning of shoot and root dry matter and carbohydrates in bean plants suffering from phosphorus, potassium and magnesium deficiency. J Exp Bot 45:1245–1250

Cakmak I, Hengeler C, Marschner H (1994b) Changes in phloem export of sucrose in leaves in response to phosphorus, potassium and magnesium deficiency in bean plants. J Exp Bot 45:1251–1257

Clarke JE, Johnson GN (2001) In vivo temperature dependence of cyclic and pseudocyclic electron transport in barley. Planta 212:808–816

Cowan JA (2002) Structural and catalytic chemistry of magnesium-dependent enzymes. Biometals 15:225–235

Dannehl H, Wietoska H, Heckmann H, Godde D (1996) Changes in D1-protein turnover and recovery of photosystem II activity precede accumulation of chlorophyll in plants after release from mineral stress. Planta 199:34–42

Fischer ES, Bremer E (1993) Influence of magnesium deficiency on rates of leaf expansion, starch and sucrose accumulation and net assimilation in *Phaseolus vulgaris*. Physiol Plant 89:271–276

Fischer ES, Lohaus G, Heineke D, Heldt HW (1998) Magnesium deficiency results in accumulation of carbohydrates and amino acids in source and sink leaves of spinach. Physiol Plant 102:16–20

Foyer CH (1988) Feedback inhibition of photosynthesis through source–sink regulation in leaves. Plant Physiol Biochem 26:483–492

Gardner RC (2003) Genes for magnesium transport. Curr Opin Plant Biol 6:263–267

Genty B, Briantais JM, Baker NR (1989) The relationship between the quantum yield of photosynthetic electron transport and quenching of chlorophyll fluorescence. Biochim Biophys Acta 990:87–92

Ghoulam C, Foursy A, Fares K (2002) Effects of salt stress on growth, inorganic ions and proline accumulation in relation to osmotic adjustment in five sugar beet cultivars. Environ Exp Bot 47:39–50

Golding A, Johnson GN (2003) Down-regulation of linear and activation of cyclic electron transport during drought. Planta 218:107–114

Hermans C, Smeyers M, Rodriguez RM, Eyletters M, Strasser RJ, Delhaye JP (2003). Quality assessment of urban trees: a comparative study of physiological characterisation, airborne imaging and on site fluorescence monitoring by the OJIP-test. J Plant Physiol 160:81–90

Igamberdiev AU, Kleczkowski LA (2001) Implications of adenylate kinase-governed equilibrium of adenylates on contents of free magnesium in plant cells and compartments. Biochem J 360:225–231

Igamberdiev AU, Kleczkowski LA (2003) Membrane potential, adenylate levels and Mg^{2+} are interconnected via adenylate kinase equilibrium in plant cells. Biochim Biophys Acta 1607:111–119

Jensen PE, Haldrup A, Rosgaard L, Scheller HV (2003) Molecular dissection of photosystem I in higher plants: topology, structure and function. Physiol Plant 119:313–321

Kaftan D, Brumfeld V, Nevo R, Scherz A, Reich Z (2002) From chloroplasts to photosystems: in situ scanning force microscopy on intact thylakoid membranes. EMBO J 21:6246–6253

Kehres DG, Maguire ME (2002) Structure properties and regulation of magnesium transport proteins. Biometals 15:261–270

Kitajima M, Butler WL (1975) Quenching of chlorophyll fluorescence and primary photochemistry in chloroplasts by dibromothymoquinone. Biochim Biophys Acta 376:105–115

Klughammer C, Schreiber U (1991) Analysis of light-induced absorbance changes in the near-infrared spectral region. I. Characterization of various components in isolated chloroplasts. Z Naturforsch Teil C 46:233–244

Kramer DM, Crofts AR (1996) Control and measurement of photosynthetic electron transport in vivo. In: Baker NR (ed.) Advances in photosynthesis: environmental stress and photosynthesis. Kluwer, Dordrecht, pp 25–66

Laing W, Greer D, Sun O, Beets P, Lowe, Payn T (2000) Pysiological impacts of Mg deficiency in *Pinus radiata*: growth and photosynthesis. New Phytol 146:47–57

Lasa B, Freschilla S, Aleu M, González-Moro B, Lamsfus C, Aparicio-Tejo PM (2000) Effects of low and high levels of magnesium on the response of sunflower plants grown with ammonium and nitrate. Plant Soil 225:167–174

Li L, Tutone AF, Drummond RSM, Gardner RC, Luan S (2001) A novel family of magnesium transport genes in *Arabidopsis*. Plant Cell 13:2761–2775

López-Bucio J, Cruz-Ramírez A, Herrera-Estrella L (2003) The role of nutrient availability in regulating root architecture. Curr Opin Plant Biol 6:280–287

Lu Y-K, Chen Y-R, Yang C-M (1995) Influence of Fe- and Mg-deficiency on the thylakoid membranes of a chlorophyll-deficient *ch5* mutant of *Arabidopsis thaliana*. Bot Bull Acad Sin 36:175–179

Marschner H (1995) Mineral nutrition of higher plants, 2nd edn. Academic Press, London

Marschner H, Kirkby EA, Cakmak I (1996) Effect of mineral nutritional status on shoot–root partitioning of photoassimilates and cycling of mineral nutrients. J Exp Bot 47:1255–1263

Mehne-Jakobs B (1995) The influence of magnesium deficiency on carbohydrate concentrations in Norway spruce (*Picea abies*) needles. Tree Physiol 15:577–584

Mengel K, Kirkby EA (1987) Principles of plant nutrition, 4th edn. International Potash Institute, Worblaufen-Bern, Switzerland, pp 481–492

Mitchell AD, Loganathan P, Payn TW, Tillman RW (1999) Effect of calcined magnesite on soil and *Pinus radiata* foliage magnesium in pumice soils of New Zealand. Aust J Soil Res 37:545–560

Oswald O, Martin T, Dominy PJ, Graham IA (2001) Plastid redox state and sugars: interactive regulators of nuclear-encoded photosynthetic gene expression. Proc Natl Acad Sci USA 98:2047–2052

Ott T, Clarke J, Birks K, Johnson GN (1999) Regulation of the photosynthetic electron transport chain. Planta 209:250–258

Paillotin G (1976) Movement of excitations in the photosynthesis domain of photosystem II. J Theor Biol 58:237–252

Pakrasi H, Ogawa T, Bhattacharrya-Pakrasi M (2001) Transport of metals: a key process in oxygenic photosynthesis. In: Aro E-M, Anderson B (eds) Regulation of photosynthesis. Kluwer, Dordrecht, pp 253–264

Pate JS, Shedley E, Arthur D, Adams MA (1998) Spatial and temporal variations in phloem sap composition of plantation-grown *Eucalyptus globules*. Oecologia 117:312–322

Peuke AD, Jeschke WD, Hartung W (2002) Flows of elements, ions and abscisic acid in *Ricinus communis* and site of nitrate reduction under potassium limitation. J Exp Bot 53:241–250

Pfeiffer W, Hager A (1993) A Ca^{2+}-ATPase and a Mg^{2+}/H^{+}-antiporter are present on tonoplast membranes from roots of *Zea mays* L. Planta 191:377–385

Porra RJ, Thompson WA, Kriedemann PE (1989) Determination of accurate extinction coefficients and simultaneous equations for assaying chlorophylls *a* and *b* extracted with four different

solvents: verification of the concentration of chlorophyll standards by atomic absorption spectrometry. Biochim Biophys Acta 975:384–394

Pujos A, Morard P (1997) Effects of potassium deficiency on tomato growth and mineral nutrition at the early production stage. Plant Soil 189:189–196

Rychter AM, Chauveau M, Bomsel J-L, Lance C (1992) The effect of phosphate deficiency on mitochondrial activity and adenylate levels in bean roots. Physiol Plant 84:80–86

Schock I, Gregan J, Steinhauser S, Schweyen R, Brennicke A, Knoop V (2000) A member of a novel *Arabidopsis thaliana* gene family of candidate Mg^{2+} ion transporters complements a yeast mitochondrial group II intron-splicing mutant. Plant J 24:489–501

Shaul O (2002) Magnesium transport and function in plants: the tip of the iceberg. Biometals 15:309–323

Shaul O, Hilgemann DW, Aldmeida-Engler J, Van Montagu M, Inzé D, Galili G (1999) Cloning and characterization of a novel Mg^{2+}/H^{+} exchanger. EMBO J 18:3973–3980

Sheen J (1990) Metabolic repression of transcription in higher plants. Plant Cell 2:1027–1038

Sokolov LN, Déjardin A, Kleczkowski LA (1998) Sugars and light/dark exposure trigger differential regulation of ADP-glucose pyrophosphorylase genes in *Arabidopsis thaliana* (thale cress). Biochem J 336:681–687

Srivastava A, Strasser RJ, Govindjee (1999) Greening of peas: parallel measurements of 77 K emission spectra, OJIP chlorophyll *a* fluorescence transient, period for oscillation of the initial fluorescence level, delayed light emission, and P700. Photosynthetica 37:365–392

Strasser RJ, Srivastava A, Govindjee (1995) Polyphasic chlorophyll *a* fluorescence transient in plants and cyanobacteria. J Photochem Photobiol 61:32–42

Sun OJ, Gielen GJHP, Tattersall Smith RSC, Thorn AJ (2001) Growth, Mg nutrition and photosynthetic activity of *Pinus radiata*: evidence that NaCl addition counteracts the impact of low Mg supply. Trees 15:335–340

Surpin M, Larkin RM, Chory J (2002) Signal transduction between the chloroplast and the nucleus. Plant Cell [Suppl] 14:327–338

Terry N, Ulrich A (1974) Effects of magnesium deficiency on the photosynthesis and respiration of leaves of sugar beet. Plant Physiol 54:379–381

Weis E, Lechtenberg D (1989) Fluorescence analysis during steady-state photosynthesis. Philos Trans R Soc Lond Ser B 323:253–268

Wilkinson SR, Welch RM, Mayland HF, Grunes DL (1990) Magnesium in plants: uptake, distribution, function and utilization by man and animals. Metal Ions Biol Syst 26:33–56

Wingler A, Mares M, Pourtau N (2004) Spatial patterns and metabolic regulation of photosynthetic parameters during leaf senescence. New Phytol 161:781–789

Wu W, Peters J, Berkowitz GA (1991) Surface charge-mediated effects of Mg^{2+} on K^{+} flux across the chloroplast envelope are associated with regulation of stromal pH and photosynthesis. Plant Physiol 97:580–587